Biochimica et Biophysica Acta, 643 (1981) 449—462
Elsevier/North-Holland Biomedical Press

BBA 79221

THE STEADY-STATE KINETIC MECHANISM OF ATP HYDROLYSIS CATALYZED BY MEMBRANE-BOUND ($Na^+ + K^+$)-ATPase FROM OX BRAIN

I. SUBSTRATE IDENTITY

LISELOTTE PLESNER [a] and IGOR W. PLESNER [b]

[a] *Institute of Biophysics and* [b] *Department of Chemistry, Physical Chemistry Division, University of Aarhus, DK-8000 Aarhus C (Denmark)*

(Received August 6th, 1980)
(Revised manuscript received November 25th, 1980)

Key words: *($Na^+ + K^+$)-ATPase; Steady-state kinetics; Substrate identity; (Ox brain)*

Summary

A detailed steady-state kinetic investigation of the hydrolysis of ATP catalyzed by ($Na^+ + K^+$)-ATPase is reported. The activity was studied in the presence of (i) Na^+ (130 mM), K^+ (20 mM) and millimolar ATP concentrations (the '($Na^+ + K^+$)-enzyme'), as well as (ii) with micromolar ATP concentrations and Na^+ (150 mM) (the 'Na^+-enzyme'). The data obtained lead to the following results:

1. The action of each enzyme may be described by a simple kinetic mechanism with one (Na^+-enzyme) or two (($Na^+ + K^+$)-enzyme) dead-end Mg complexes.

2. For both enzymes, both MgATP and free ATP are substrates, with Mg^{2+}, in the latter case, as the second substrate.

3. For each enzyme, the complete set of kinetic constants (seven for the Na^+-enzyme, eight for the ($Na^+ + K^+$)-enzyme) are determined from the data.

4. For each enzyme it is shown that, in the alternate substrate mechanism obtained, the ratio of net steady-state flux along the 'MgATP pathway' to that of the 'ATP-Mg pathway' increases linearly with the concentration of free Mg^{2+}. The parameters of this function are determined from the data. As a result of this, at high (greater than 3 mM) free Mg^{2+} concentrations the alternate substrate mechanism degenerates into a 'limiting' kinetic mechanism, with MgATP as the (essentially) sole substrate, and Mg^{2+} as an uncompetitive (Na^+-enzyme) or non-competitive (($Na^+ + K^+$)-enzyme) inhibitor.

Introduction

Despite intensive efforts since the establishment by Skou [1] of the intimate connection between the cation transport system in membranes and an ATPase stimulated by Na^+, K^+ and Mg^{2+} (adenosine-5′-triphosphatase, EC 3.6.1.3), a number of fundamental questions concerning the action of the enzyme are still unanswered.

One of these is the precise identity of the substrate: is it MgATP or ATP? This question has been studied by Hexum et al. [2] and also by Robinson [3]. In both of these studies, it is concluded that MgATP is the sole substrate, while ATP is a competitive and Mg^{2+} is an uncompetitive [2] or a non-competitive [3] inhibitor. In the first of these studies [2], the conclusion is based on the property that if the apparent K_m for ATP_{free} at one concentration of Mg^{2+}_{free} equals the apparent K_m for Mg^{2+}_{free} at the same concentration of ATP_{free}, then the complex MgATP is the true substrate. This property, however, obtains (in a strict sense) only when none of the other ligands (ATP_{free} or Mg^{2+}_{free}) appreciably affects the enzyme.

The conclusion that only MgATP is the substrate is inconsistent with the fact (Klodos, I., personal communication; see also Refs. 4 and 23) that ATP when bound to the enzyme without Mg^{2+}, upon the addition of Mg^{2+} phosphorylates the enzyme. Nor do the conclusions, referred to above, explain the differential action of Mg^{2+}, depending on its concentration [5] or the complex results obtained by Skou [6].

In the present article, the first in a series dealing with the kinetic mechanism of $(Na^+ + K^+)$-ATPase, the steady-state kinetics of the bovine brain enzyme were studied at pH 7.4. We have been concerned only with the interaction of the enzyme with the ligands Mg^{2+}, ATP, and MgATP — the detailed kinetic effects of Na^+ and K^+ were not studied.

It will be shown that our kinetic results lead to a fairly simple steady-state mechanism for the action of both enzymes. The mechanism is sufficiently simple to allow the derivation of the complete rate equation without making assumptions about equilibrium among the states in the mechanism. Yet, the resulting equations, when taking account of the prevailing equilibrium between Mg^{2+}, ATP and MgATP, are sufficiently complex to account for all the kinetic patterns observed. In addition, with a steady-state mechanism we can distinguish whether MgATP or $(ATP + Mg^{2+})$ or both are substrates, which is not possible if equilibrium conditions are imposed on the mechanism [7].

Materials and Methods

The $(Na^+ + K^+)$-ATPase was a gift from I. Klodos and prepared from ox brain as described previously by Klodos et al. [8] (see also paper II of this series [28]. The activity of the enzyme measured with 3 mM ATP, 130 mM NaCl, 20 mM KCl, 3 mM $MgCl_2$ and 30 mM histidine buffer, pH 7.4, at 37°C was 2.6 μM ATP hydrolysed/mg protein per min. Less than 1% of the activity was Mg^{2+}-activated ATPase (measured in the presence of $1 \cdot 10^{-3}$ M g-strophantin).

Assay of the $(Na^+ + K^+)$-enzyme. The enzyme preparation containing 2 mg protein ml^{-1} was diluted 26—51-times for the kinetic experiments. A further

dilution of 10-times took place in the assays which were performed at pH 7.4 in a 30 mM histidine buffer and in the presence of 130 mM NaCl and 20 mM KCl at varying concentrations of the disodium salt of ATP (Boehringer) and $MgCl_2$. The temperature of the assay was 37°C. An individual blind was run for each tube and it was assured that under each set of conditions the reaction rate was constant within the assay time. P_i was measured according to the method of Ottolenghi [9].

Assay of the Na^+-enzyme. For these experiments, both the disodium salt of ATP from Boehringer as well as [γ-^{32}P]ATP (triethylammonium salt) from Amersham were purified on DEAE-Sephacel. The column was equilibrated in 30 mM Tris-HCl, pH 9.6, and after rinsing of the column with 30 mM histidine buffer, pH 7.4, ATP was eluted by an NaCl gradient in this buffer. Elution took place at 125 mM NaCl. The enzyme preparation was diluted 1000-times for the kinetic experiments and a further dilution of 10-times took place in the assays, performed at pH 7.4 in the presence of 30 mM histidine, 150 mM NaCl and at varying concentrations of $MgCl_2$ and [γ-^{32}P]ATP (specific activity $2—11 \cdot 10^6$ cpm $\cdot$ nmol^{-1}).

The velocity of ATP hydrolysis at 37°C was measured by using the method of Lindberg and Ernster [10]. An individual blind was run for each tube and it was assured that under each set of conditions the reaction rate was constant within the assay time.

The dissociation constant, K_T, for the MgATP complex was measured according to the method of Burton [11] using the spectral changes of 8-hydroxyquinoline to determine the amount of free bivalent metal ion present in solution containing ATP. A 4 cm light-path quartz cuvette fitted with temperature control and stirring device was used, and the measurements were carried out at 37°C with buffer, NaCl and KCl concentrations identical to those in the kinetic experiments. Under these circumstances, the value obtained was $K_T = 0.085$ mM.

Reproducibility. In estimating errors of quantities such as slopes and intercepts of regression lines (which in turn have been used as the basis for weighting), we have chosen to indicate (in the legends to figures) the (relative) actual deviations (sometimes average deviations) of individual determinations from their corresponding means, rather than the calculated standard errors. This would be particularly relevant in cases where an average of only two to three determinations is used, since the calculated standard error in such cases is known to be a rather poor estimate of the statistic σ. Our main objective in this work has been to establish compatibility between the model and the observed kinetic patterns.

Results and Discussion

The usual procedure in steady-state kinetic experiments, when one wishes to investigate the nature of the interaction between several ligands and the enzyme, is to vary one ligand concentration at several fixed levels of the others. Because Mg^{2+} and ATP in solution form the complex MgATP in equilibrium with its constituents:

$$MgATP \rightleftharpoons Mg^{2+} + ATP \qquad (1)$$

the three concentrations $[Mg^{2+}_{free}]$, $[ATP_{free}]$ and [MgATP] cannot be varied independently. We can, however, study the enzyme at a series of constant concentrations of one of the three possible ligands.

In the experiments reported here, the steady-state rate of hydrolysis was measured as a function of the MgATP concentration at various fixed levels of $[Mg^{2+}_{free}]$.

The data were plotted (in double-reciprocal form) using either $[MgATP]^{-1}$ or $[ATP_{free}]^{-1}$ as the abscissa. From the patterns so obtained, together with secondary plots of slopes and ordinate intercepts as functions of $[Mg^{2+}_{free}]$ or $[Mg^{2+}_{free}]^{-1}$, the kinetic mechanism may be deduced.

In what follows we shall speak of the $(Na^+ + K^+)$-enzyme as the enzyme when studied in the presence of both Na^+ and K^+ ($[K^+]$ = 20 mM, $[Na^+]$ = 130 mM) and with millimolar concentrations of MgATP, and of the Na^+-enzyme when only micromolar MgATP concentrations (and Na^+) are present.

I. The $(Na^+ + K^+)$-enzyme

The data from four representative kinetic runs at various fixed levels of $[Mg^{2+}_{free}]$ are presented in Figs. 1 and 2, using $[MgATP]^{-1}$ and $[ATP_{free}]^{-1}$,

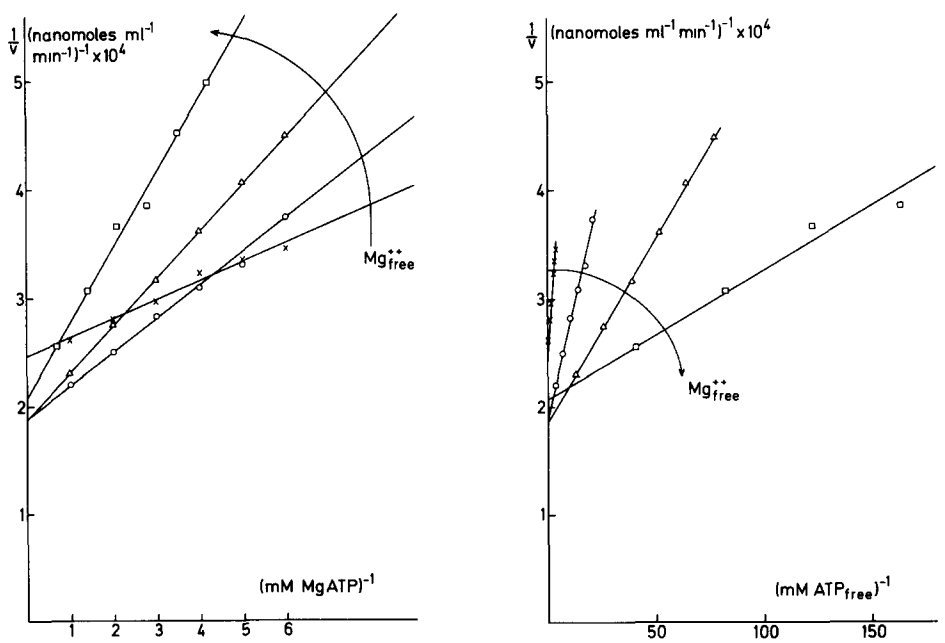

Fig. 1. Kinetic data for the $(Na^+ + K^+)$-enzyme. For clarity, only four runs (out of 26 runs used for slope and intercept determination (Figs. 3 and 4)) at various, constant, Mg^{2+} concentrations are presented in double-reciprocal form, using $[MgATP]^{-1}$ as abscissa. The rate measurements are normalized to correspond to the undiluted enzyme (2 mg protein/ml). $[Na^+]$ = 130 mM, $[K^+]$ = 20 mM, pH 7.4, 37° C. Concentrations of free Mg^{2+}: 0.06 mM (X), 0.3 mM (○); 1.1 mM (△); 5.0 mM (□). The lines are the least-squares regression lines.

Fig. 2. The data from Fig. 1 plotted vs. $[ATP_{free}]^{-1}$. $[Mg^{2+}_{free}]$: 0.06 mM (X); 0.3 mM (○); 1.1 mM (△); 5.0 mM (□).

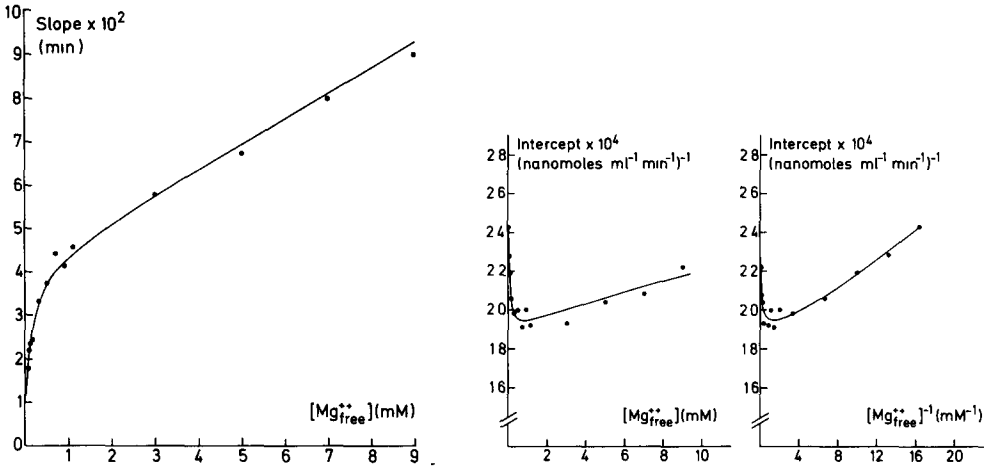

Fig. 3. Slopes of lines (v^{-1} vs. $[MgATP]^{-1}$, as in Fig. 1) vs. $[Mg^{2+}_{free}]$. Each point is an average of two determinations, differing by less than 10%. The curve drawn is the weighted least-squares fit of the slope function in Eqn. 5 to the data (see Appendix).

Fig. 4. Vertical intercepts of lines (v^{-1} vs. $[MgATP]^{-1}$, as in Fig. 1) vs. (a) $[Mg^{2+}_{free}]$ and (b) $[Mg^{2+}_{free}]^{-1}$. Each point is an average of two determinations differing by less than 10%. The curves are the weighted least-squares fit of the intercept term in Eqn. 5 to the data (see Appendix).

respectively, as abscissa. We observe in both cases families of straight lines which do not cross in a single point.

In Figs. 3 and 4a are plotted the slopes and vertical intercepts obtained from lines like those in Fig. 1 as a function of $[Mg^{2+}_{free}]$.

As mentioned in the Introduction, the kinetic results reported hitherto [3] were interpreted to correspond to a mechanism in which MgATP was the sole substrate, and Mg^{2+}_{free} and ATP_{free} were non-competitive and competitive inhibitors, respectively *:

$$\begin{array}{lcl} & \text{EMg} \quad \text{EMgATPMg} & \\ K_{OM} \updownarrow & \qquad \updownarrow K_{MM} & \\ \text{E} & \rightleftharpoons \text{EMgATP} \rightarrow \text{E} + \text{products} & \\ K_{iA} \updownarrow & & \\ \text{EATP} & & \end{array} \qquad \text{(I)}$$

The steady-state reciprocal initial rate for this mechanism is ($MA \equiv [MgATP]$, $A \equiv [ATP_{free}]$, $M \equiv [Mg^{2+}_{free}]$):

$$\frac{1}{v} = \frac{1}{V_{MA}}\left\{\frac{K_{MA}}{MA}\left(1 + \frac{A}{K_{iA}} + \frac{M}{K_{OM}}\right) + 1 + \frac{M}{K_{MM}}\right\} \qquad (2)$$

* Following Cleland [12], we characterize an inhibitor as uncompetitive, competitive, or non-competitive, according to whether it influences the (ordinate) intercept, the slope, or both, respectively, in a double-reciprocal plot of the data.

where K_{MA} and V_{MA} are the Michaelis constant and maximal velocity, respectively, and K_{OM}, K_{MM} and K_{iA} are the equilibrium (dissociation) constants indicated in mechanism I.

In order to compare this equation with the data exhibited in Fig. 1 or Fig. 2 (where M, for any line, is constant), we must eliminate either A (for Fig. 1) or MA (for Fig. 2) from Eqn. 2, using the relationship:

$$K_T = \frac{M \cdot A}{MA} \tag{3}$$

We obtain:

$$\frac{1}{v} = \frac{K_{MA}}{V_{MA}}\left(1 + \frac{M}{K_{OM}}\right)\frac{1}{MA} + \frac{1}{V_{MA}}\left(1 + \frac{K_{MA}K_T}{K_{iA}}\right)\frac{1}{M} + \frac{M}{K_{MM}} \tag{4a}$$

$$= \frac{K_{MA}K_T}{V_{MA}}\left(\frac{1}{K_{OM}} + \frac{1}{M}\right)\frac{1}{A} + \frac{1}{V_{MA}}\left(1 + \frac{K_{MA}K_T}{K_{iA}} \cdot \frac{1}{M} + \frac{M}{K_{MM}}\right) \tag{4b}$$

When considering Eqns. 4a and b it is seen that these expressions go a long way towards explaining the data presented in Figs. 1—4:

(i) The reciprocal rate is linear in the reciprocal MA or A concentration, Eqns. 4a and b;

(ii) the intercept in Eqn. 4a ($= 1/V_{MA}\ (1 + K_{MA}K_T/K_{iA} \cdot 1/M + M/K_{MM})$ is linear in M at large M (Fig. 4a) and linear in $1/M$ at small M (Fig. 4b);

(iii) the slope ($= K_{MA}/V_{MA}\ (1 + M/K_{OM})$) is linear in M (Fig. 3, $M > 3$ mM), and

(iv) it may be shown that Eqns. 4a and b are consistent with the observed property that if two lines (at M_1 and M_2) in Fig. 1 intersect to the left of the ordinate axis, the corresponding lines (same M_1 and M_2) in Fig. 2 will intersect to the right of the ordinate.

However, it will be noted that the possibility of resolving the slope as a function of M in two straight lines with different slopes (cf. Fig. 3) is not accounted for by Eqn. 4a.

In order to explain this feature by a modification of the model shown above, we can derive rate equations for the possible single-substrate models in which either ATP_{free} or MgATP is the substrate, and the remaining two ligands are either non-competitive or competitive inhibitors or essential activators. When the rate equations so obtained (after elimination of $[ATP_{free}]$ or [MgATP]) are compared with the relevant data, it is seen that the feature exhibited in Fig. 3 cannot described by this class of model with only a single substrate.

The simplest alternative mechanism which has the desired properties is shown in Fig. 5. Here, ATP + Mg^{2+}, in that order, are alternate substrates to MgATP, and, in addition, Mg^{2+} also forms inactive complexes with the substrate-free enzyme E and with the enzyme-substrate complexes EMA. The latter are assumed to have the same breakdown rate constant k_2 and are identical if (a) Mg^{2+} does not distinguish between ATP free and bound to the enzyme (i.e., $K_T = k_{-2}/k'_2$) and (b) the enzyme does not distinguish between $(ATP)_{free}$ and MgATP (i.e., $k'_{-1}/k'_1 = k_{-1}/k_1$). We retain their distinction in Fig. 5 in order to keep track of the fluxes along the two pathways (see below).

Using the diagram method of King and Altman [13], the complete steady-

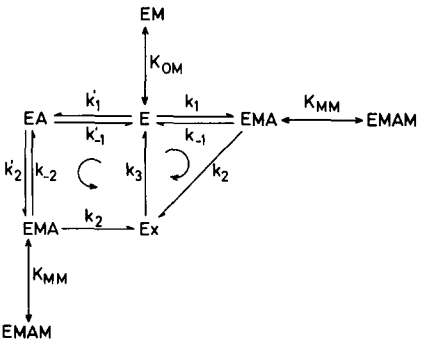

Fig. 5. Kinetic model for the ($Na^+ + K^+$)-enzyme and (when omitting the species EM, see text) for the Na^+-enzyme. k_i and k'_i are rate constants, K_{MM} and K_{OM} are dissociation constants. Double-headed arrows indicate equilibrium. The curved arrows indicate the positive direction of the net steady-state flux in each cycle (see text).

state rate equation in terms of rate constants may be derived. From this we define, using the systematic procedure of Cleland [14] (see also Ref. 27), the kinetic constants shown in Table I. When these are inserted in the rate equation, and A is eliminated, using Eqn. 3, as before, we finally obtain for the reci-

TABLE I

DEFINITIONS OF KINETIC CONSTANTS FOR THE MECHANISM (Fig. 5) USED IN EQN. 5

In deriving this equation, the relationship $K_{iA}K_M = K_{iM}K_A$ has been used.

Quantity	Definitions in terms of rate constants and concentrations
r	$r = k_3/(k_2 + k_3)$
Maximum velocity	$V_{MA} = k_2k_3E_o/(k_2 + k_3) = r \cdot k_2E_o$
Michaelis constant for MgATP	$K_{MA} = \frac{(k_{-1} + k_2)k_3}{k_1(k_2 + k_3)} = r \cdot \frac{k_{-1} + k_2}{k_1}$
Michaelis constant for Mg	$K_M = \frac{(k_{-2} + k_2)k_3}{k'_2(k_2 + k_3)} = r \cdot \frac{k_2 + k_{-2}}{k'_2}$
Michaelis constant for ATP	$K_A = \frac{k_2k_3}{k'_1(k_2 + k_3)} = r \cdot \frac{k_2}{k'_1}$
Dissociation constant for EATP	$K_{iA} = \frac{k'_{-1}}{k'_1}$
Product inhibition constant for Mg	$K_{iM} = \frac{k'_{-1}(k_{-2} + k_2)}{k'_2k_2}$
Dissociation constant for enzyme-Mg complex K_{MM}, K_{OM}	See Fig. 5
Dissociation constant for MgATP	$K_T = \frac{[Mg^{2+}_{free}] \cdot [ATP_{free}]}{[MgATP]}$
Q	$Q \equiv \frac{K_TK_{MA}}{K_{iA}K_M}$

procal rate:

$$v^{-1} = \frac{K_{MA}}{V_{MA}} \cdot \frac{(1 + M/K_{iM})(1 + M/K_{OM})}{1 + Q + M/K_{iM}} \cdot (MA)^{-1} + V_{MA}^{-1}\left[1 + M/K'_{MM} + \frac{K_T K_{MA}/K_{iA}}{1 + Q + M/K_{iM}} \cdot M^{-1}\right] \quad (5)$$

where $Q = K_T K_{MA}/K_{iA}K_M$, $K'_{MM} = K_{MM}/r$, and $r = k_3/(k_2 + k_3)$.

If $K_{OM} > K_{iM}$, Eqn. 5 is consistent with points i–iv above and, in addition, Eqn. 5 will explain the two different slopes of the line in Fig. 3.

At large M ($M/K_{iM} >> 1 + Q$), the slope, from Eqn. 5, of v^{-1} vs. $1/MA$ is just $K_{MA}(1 + M/K_{OM})/V_{MA}$, which is a linear function of M with slope $K_{MA}/K_{OM}V_{MA}$. The intercept from Eqn. 5 at these M values is $V_{MA}^{-1}(1 + M/K'_{MM})$, corresponding to Fig. 4a.

At small M ($M/K_{iM} << 1 + Q$), the slope, from Eqn. 5, is essentially $K_{MA} \cdot (1 + M/K_{iM})/V_{MA}(1 + Q)$, which also is a linear function of M, but the slope of this line is $K_{MA}/V_{MA}K_{iM}(1 + Q)$. The intercept from Eqn. 5 is slightly more complex than before, but at sufficiently small M it becomes linear in M^{-1} with slope $K_T K_{MA}/V_{MA}(1 + Q)K_{iA}$.

It may be shown that compatibility with the data, as described above, cannot be obtained if Mg^{2+} is the first, and ATP the second, substrate along the alternate substrate path.

We therefore conclude that the simplest kinetic scheme compatible with all the data is the mechanism shown in Fig. 5, and that Mg^{2+} is both an activator (being a second substrate) and a dead-end inhibitor.

Using Eqn. 5, the kinetic constants for the ($Na^+ + K^+$)-enzyme may be deter-

TABLE II

VALUES OF KINETIC PARAMETERS DETERMINED FROM THE DATA

K_T is the dissociation constant for MgATP: $K_T = 85 \pm 2$ μM. Values are given ± S.D. (see Appendix). For definition and significance of constants, see Table I.

	($Na^+ + K^+$)-enzyme	Na^+-enzyme
V^*_{MA} (nmol · ml^{-1} · min^{-1})	5208 ± 90	186 ± 5
K_{OM} (μM)	(7.6 ± 0.5) · 10^3	∞
K_{MA} (μM)	224 ± 6	0.69 ± 0.02
K_M (μM)	28 ± 10	11 ± 3
K_{iM} (μM)	39 ± 17	53 ± 1
K_{iA} (μM)	202 ± 35	0.76 ± 0.18
K_A (μM)	145 ± 77	0.16 ± 0.03
$K'_{MM} = \frac{K_{MM}}{r}$ (μM)	(66 ± 8) · 10^3	(38 ± 4) · 10^3
$Q = \frac{K_T K_{MA}}{K_{iA} K_M}$	3.3 ± 1.0	7.1 ± 0.8

* The undiluted enzyme preparation contained 2 mg protein/ml. Correspondingly, the maximal specific activities are 2600 and 90 nmol · mg^{-1} . min^{-1} for the two enzymes, respectively. The reason for the somewhat unusual units in the table is that, with these, the concentration unit in the value of V_{MA} is the same as that used in the kinetic constants (μM).

mined from the data. The procedure for this is detailed in the Appendix. The values are presented in Table II.

The enzyme-ATP dissociation constant K_{iA} is 0.2 mM. This is in agreement with the value found by Grosse et al. [15]: 0.24 ± 0.03 mM at 37°C. Other existing estimates of this quantity are that of Robinson [16] (approx. 0.4 mM at 0°C) and that of Karlish and Yates [17] (approx. 0.45 at 20°C).

We note that the Michaelis constant for ATP, K_A, is slightly smaller than K_{iA}, while the Michaelis constant for MgATP, K_{MA}, is almost equal to K_{iA}. This makes it possible to attach a physical significance to the quantity Q defined in Eqn. 5 (see also Table I): If $K_{iA} \simeq K_{MA}$, we have:

$$Q \simeq K_T/K_M$$

Q is thus a measure of the ability of Mg^{2+} to act as a substrate ($\sim 1/K_M$), relative to its effectiveness as a complexing agent for ATP ($\sim 1/K_T$).

The relationship between the kinetic constants and the individual rate constants are too complex (see Table I) to render a determination of the latter possible on the basis of our experiments. Nor can the intrinsic inhibition constant K_{MM} for Mg^{2+} be computed, since the apparent value, K'_{MM}, contains the unknown rate constant ratio r. Operationally, Mg^{2+} inhibits the enzyme-substrate complex only very weakly ($K'_{MM} \simeq 66$ mM), whereas a somewhat stronger inhibition of the substrate-free enzyme form is observed ($K_{OM} = 7.6$ mM).

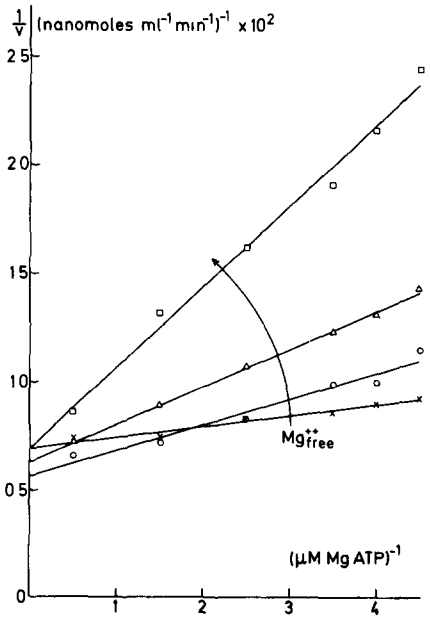

Fig. 6. Double-reciprocal plot of the kinetic data for the Na^+-enzyme at various constant Mg^{2+} concentrations. Four runs (out of a total of 46 runs used for slope and intercept determination (Figs. 7 and 8)) are presented. Abscissa: $[MgATP]^{-1}$. The rate measurements were normalized to correspond to the undiluted enzyme (2 mg protein/ml). $[Na^+]$ = 150 mM, pH 7.4, 37°C. $[Mg^{2+}_{free}]$: 0.04 mM (×); 0.1 mM (○); 0.3 mM (△); 12 mM (□). The lines are the least-squares regression lines.

II. The Na^+-enzyme

The data, in double-reciprocal form, are presented in Fig. 6, while slopes and vertical intercepts as functions of M are shown in Figs. 7 and 8. Again, the intercept, at small M, appears linear in M^{-1} (not shown).

We note that, at large M, the slope is a constant, independent of M, in contrast to the $(Na^+ + K^+)$-enzyme discussed above. Hence, at these values of M, Mg^{2+} shows uncompetitive inhibition. Apart from this feature, resulting in the lack of the term $(1 + M/K_{OM})$ in the slope term of Eqn. 5, the argument proceeds along the same lines as set forth above. Hence, we conclude that the kinetic mechanism is the same for this enzyme as for the $(Na^+ + K^+)$-enzyme, except that Mg^{2+} in this case does not bind to the substrate-free enzyme form. Thus, the complete steady-state rate is again Eqn. 5, but with $K_{OM} = \infty$.

From the data the kinetic constants may be determined as before (see Appendix). The values are tabulated in Table II.

The value of the dissociation constant for the enzyme-ATP complex is here $K_{iA} = 0.76$ μM. Grosse et al. [15] found 5 ± 3 μM at 37°C for the high-affinity site of the enzyme. At other temperatures, the values obtained are: 0.13 μM [18] and 0.2 μM [19] at 0°C, and 0.15 μM [20] at 20°C. We note that in this case the Michaelis constant, $K_A = 0.16$ μM, is smaller than K_{iA} by a factor of 5. The apparent inhibition constant for Mg^{2+}, K'_{MM}, is 38 mM. Again, since $K_{MA} \simeq K_{iA}$, we have $Q \simeq K_T/K_M$. For this enzyme the 'relative efficiency' of Mg^{2+} as a substrate is about twice as large as for the $(Na^+ + K^+)$-enzyme.

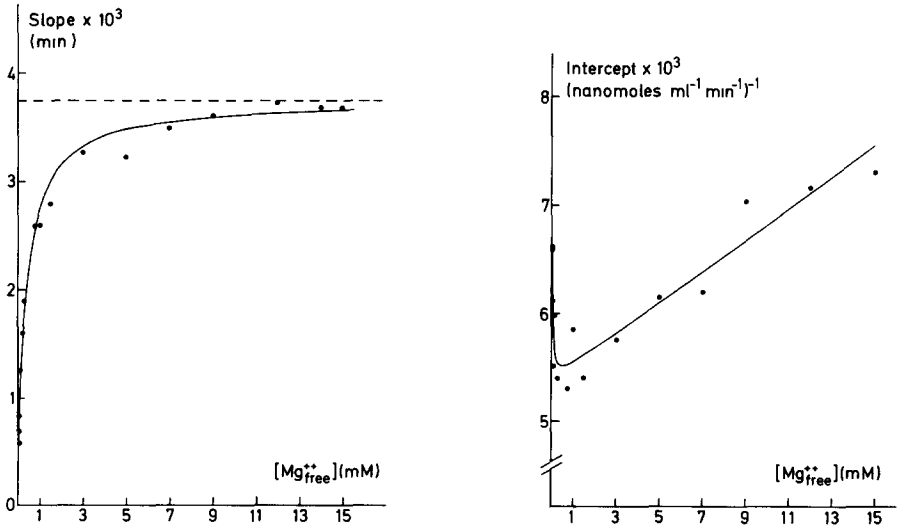

Fig. 7. The slopes of lines (v^{-1} vs. $[MgATP]^{-1}$, as in Fig. 6) as a function of $[Mg^{2+}_{free}]$. Each point is an average of two to seven determinations (a total of 46 values). The average deviation of any individual determination from the corresponding mean was less than 7%. The curve and the horizontal dashed line are obtained from a weighted least-squares fit of Eqn. A1 to the data (see Appendix).

Fig. 8. Vertical intercepts of lines (v^{-1} vs. $[MgATP]^{-1}$, as in Fig. 6) as a function of $[Mg^{2+}_{free}]$. Each point is an average of two to seven determinations, the average deviation of which from the mean was less than 8%. The curve is that obtained from a weighted least-squares fit of Eqn. A2 to the data (see Appendix).

III. Flux ratio

For each enzyme we can estimate the importance of the 'MgATP-cycle' (E-EMA-Ex-E) relative to the 'ATP-Mg-cycle' (E-EA-EMA-Ex-E), by calculating the ratio of net steady-state fluxes along the two pathways. Using the flux diagram technique of Hill [21] for the mechanism shown in Fig. 5 (positive direction of net flux is indicated by curved arrows in each cycle) we obtain, using the definitions in Table I:

$$R \equiv \frac{J_{\mathrm{MgATP}}}{J_{\mathrm{ATP\text{-}Mg}}} = \left(1 + \frac{M}{K_{1\mathrm{M}}}\right)/Q \tag{6}$$

where the J values are the net steady-state fluxes under the conditions of the experiment (i.e., with no products present). Using the values for the constants in each case (Table II) we obtain:

$$R((\mathrm{Na^+} + \mathrm{K^+})\text{-enzyme}) = (1 + M/0.039)/3.3 \tag{7}$$

$$R(\mathrm{Na^+}\text{-enzyme}) = (1 + M/0.053)/7.1 \tag{8}$$

(with M in the units mM). The two cycles are equally important ($R = 1$) at M = 0.09 mM and M = 0.32 mM, respectively. For M = 3 mM, the ratios are

$$R((\mathrm{Na^+} + \mathrm{K^+})\text{-enzyme}) \simeq 23.6 \tag{9}$$

$$R(\mathrm{Na^+}\text{-enzyme}) \simeq 8.1 \tag{10}$$

At this concentration of $\mathrm{Mg^{2+}_{free}}$, for both enzymes, the MgATP-cycle accounts for about 90% or more of the total flux. This is probably responsible for the previous findings that only MgATP is a substrate for the reaction [2,3]. A similar conclusion, that MgATP is the only substrate, was reported also by Epstein and Whittam [22].

It is interesting to point out that, as seen from Figs. 4 and 8, the maximal activity of both enzymes is obtained with $[\mathrm{Mg^{2+}_{free}}] \approx 1$ mM. This is in accord with the observation by Skou [6] that maximal activity of the enzyme, with [ATP] = 3 mM, is obtained when $[\mathrm{Mg^{2+}}]$: [ATP] = 4 : 3 *. At this concentration of $\mathrm{Mg^{2+}_{free}}$, we have:

$$R((\mathrm{Na^+} + \mathrm{K^+})\text{-enzyme}) = 8$$

$$R(\mathrm{Na^+}\text{-enzyme}) = 2.8$$

i.e., 89 and 74%, respectively, of the fluxes (in each cycle) are along the MgATP pathway in the two cases.

IV. Concluding remarks

The enzyme intermediate Ex left unspecified in Fig. 5 is not kinetically distinguishable, i.e., the rate equation obtained when omitting Ex from the model is identical in form with Eqn. 5, and the definitions, in terms of rate constants, are those in Table I with $r = 1$ **. We include Ex in the model because it is

---

* We are grateful to a referee for point this out.

** This purely formal procedure is valid providing the rate constant leading back to the empty enzyme E under release of product (P_i) is denoted k_2.

known, for the Na^+-enzyme, that (phosphorylated) intermediates exist.

With the results reported here we believe to have clarified the interaction of the two enzymes (the $(Na^+ + K^+)$-enzyme and the Na^+-enzyme, as operationally defined above) with ATP, Mg^{2+} and MgATP. The two mechanisms obtained, though almost identical in form, are characterized by very different sets of kinetic constants.

On the other hand, it is generally accepted that the $(Na^+ + K^+)$-ATPase is a single enzyme which, depending on the substrate concentration, and the monovalent cation composition of the medium, exhibits '$(Na^+ + K^+)$-enzyme activity' or 'Na^+-enzyme activity'. With the characterization of these two activities at hand, it thus becomes a task to combine them into a single model for the overall hydrolytic action of $(Na^+ + K^+)$-ATPase.

Such a model, an extended and somewhat elaborated version of the Post-Albers scheme [23,24], has been suggested recently by Karlish et al. [25]. We derive in paper III of this series [29] a rate constant condition which must be met, if such a scheme is to exhibit a ratio of maximal velocities for the two activities of about 25, as determined above (see Table II). The application of this condition requires a detailed analysis of kinetic data for the dephosphorylation of the phosphorylated enzyme, which is the subject of the following paper [28]. On the basis of these results, and on data for K^+ inhibition of the Na^+-enzyme, presented in paper III [29], we shall propose a (minimal) model for the hydrolytic action of $(Na^+ + K^+)$-ATPase.

Appendix

Determination of kinetic constants

We define $S(M)$ and $I(M)$ by the equations:

$$S(M) = \frac{K_{MA}}{V_{MA}} \frac{(1 + M/K_{iM})}{1 + Q + M/K_{iM}} \tag{A1}$$

$$I(M) = V_{MA}^{-1}\left[1 + \frac{M\ r}{K_{MM}} + \frac{K_T K_{MA} K_{iA}^{-1}}{1 + Q + M/K_{iM}} \cdot M^{-1}\right] \tag{A2}$$

Eqn. 5 may then be written:

$$v^{-1} = S(M)(1 + M/K_{OM}) \cdot (MA)^{-1} + I(M) \tag{A3}$$

(a) *The Na^+-enzyme: $K_{OM} = \infty$*

The function:

$$S = A(1 + CM)/(1 + B + CM) \tag{A4}$$

is first fitted to the slope data (Fig. 7) using a non-linear, weighted least-squares curve-fitting computer routine. The resulting values of A, B and C then yield:

$$K_{MA}/V_{MA} = A \tag{A5}$$

$$Q = B \tag{A6}$$

$$K_{iM} = 1/C \tag{A7}$$

With the values for Q and K_{iM} so obtained, the function:

$$I = D + F \cdot M + \frac{G}{(1 + Q)\,M + M^2/K_{iM}} \tag{A8}$$

is fitted to the data for the intercept (Fig. 8). We now have (cf. Eqn. A2):

$$V_{MA} = 1/D \tag{A9}$$

$$K'_{MM} \equiv K_{MM}/r = D/F \tag{A10}$$

$$K_{iA} = K_T \cdot A/G \tag{A11}$$

where K_T is the dissociation constant for the MgATP complex. The remaining kinetic constants are then calculated using the relationship (cf. Eqns. A1 and A2 and Table I)

$$K_{MA} = A/D \tag{A12}$$

$$K_M = \frac{G}{D \cdot B} \tag{A13}$$

$$K_A = \frac{K_{iA} \cdot K_M}{K_{iM}} = K_T \cdot \frac{A \cdot C}{D \cdot B} \tag{A14}$$

The curves drawn in Figs. 7 and 8 are calculated from Eqns. A1 and A2, using the fitted sets of constants A, B, C, and D, F, G, respectively. The values obtained for the kinetic constants are tabulated in Table II.

The standard deviations of the fitted constants are calculated from the weighted least-squares fitting procedure. From these are calculated the standard errors of the kinetic constants, using standard formulae for the propagation of errors [26].

(b) The (Na^+ + K^+)-enzyme

In this case, the linear part of the slope for $M \geqslant 3$ mM is first used to calculate K_{OM}. The data for the slope (Fig. 3) are divided by $(1 + M/K_{OM})$, resulting in a set of data, to which should be fitted a function of the form $S(M)$ (Eqn. A1). These data as well as those for the intercept (Fig. 4) are then treated as in case (a) above. The curves drawn in Figs. 3 and 4 are again those calculated for the slope and intercept of Eqn. A3, using the fitted sets of constants.

Acknowledgements

We wish to express our gratitude to J.C. Skou, I. Klodos and J.G. Nørby for numerous discussions and constructive criticism. We thank Mrs. Vinni Ravn for her meticulous care with and constant interest in the experiments. This work was supported by a grant from the Danish Medical Research Council, J. No. 512-10806.

References

1 Skou, J.C. (1957) Biochim. Biophys. Acta 23, 394—402
2 Hexum, T., Samson, F.E., Jr. and Himes, R.H. (1970) Biochim. Biophys. Acta 212, 322—331

3 Robinson, J.D. (1974) Biochim. Biophys. Acta 341, 233—247
4 Mårdh, S. and Post, R.L. (1977) J. Biol. Chem. 252, 633—638
5 Robinson, J.D. and Flashner, M.S. (1979) in Na,K-ATPase: Structure and Kinetics (Skou, J.C. and Nørby, J.G., eds.), pp. 275—285, Academic Press, London
6 Skou, J.C. (1974) Biochim. Biophys. Acta 339, 234—273
7 Wang, T., Lindenmayer, G.E. and Schwartz, A. (1977) Biochim. Biophys. Acta 484, 140—160
8 Klodos, I., Ottolenghi, P. and Boldyrev, A.A. (1975) Anal. Biochem. 67, 397—403
9 Ottolenghi, P. (1975) Biochem. J. 151, 61—66
10 Lindberg, O. and Ernster, L. (1956) in Methods of Biochemical Analysis (Gliek, G., ed.), Vol. 3, pp. 1—22, Interscience, New York
11 Burton, K. (1959) Biochem. J. 71, 388—395
12 Cleland, W.W. (1963) Biochim. Biophys. Acta 67, 173—187
13 King, E.L. and Altman, C. (1956) J. Phys. Chem. 60, 1375
14 Cleland, W.W. (1963) Biochem. Biophys. Acta 67, 104—137
15 Grosse, R., Eckert, K., Malur, J. and Repke, K.R.H. (1978) Acta Biol. Med. Ger. 37, 83—96
16 Robinson, J.D. (1976) Biochim. Biophys. Acta 429, 1006—1019
17 Karlish, S.J.D. and Yates, D.W. (1978) Biochim. Biophys. Acta 527, 115—130
18 Nørby, J.G. and Jensen, J. (1971) Biochim. Biophys. Acta 233, 104—116
19 Hegyvary, C. and Post, R.L. (1971) J. Biol. Chem. 246, 5234—5240
20 Karlish, S.J.D., Yates, D.W. and Glynn, I.M. (1976) Nature 263, 251—253
21 Hill, T.L. (1977) Free Energy Transduction in Biology, Academic Press, New York
22 Epstein, F.H. and Whittam, R. (1966) Biochem. J. 99, 232—238
23 Albers, R.W. (1967) Annu. Rev. Biochem. 36, 727—756
24 Post, R.L., Kume, S., Tobin, T., Orcutt, H.B. and Sen, A.K. (1969) J. Gen. Physiol. 54, 306S—326S
25 Karlish, S.J.D., Yates, D.W. and Glynn, I.M. (1978) Biochim. Biophys. Acta 525, 252—264
26 Bevington, Philip R. (1969) Data Reduction and Error Analysis for the Physical Sciences, McGraw-Hill, New York
27 Segel, I.H. (1975) Enzyme Kinetics, pp. 523—530, Wiley and Sons, New York
28 Klodos, I., Nørby, J.G. and Plesner, I.W. (1981) Biochim. Biophys. Acta 643, 463—482
29 Plesner, I.W., Plesner, L., Nørby, J.G. and Klodos, I. (1981) Biochim. Biophys. Acta 643, 483—494